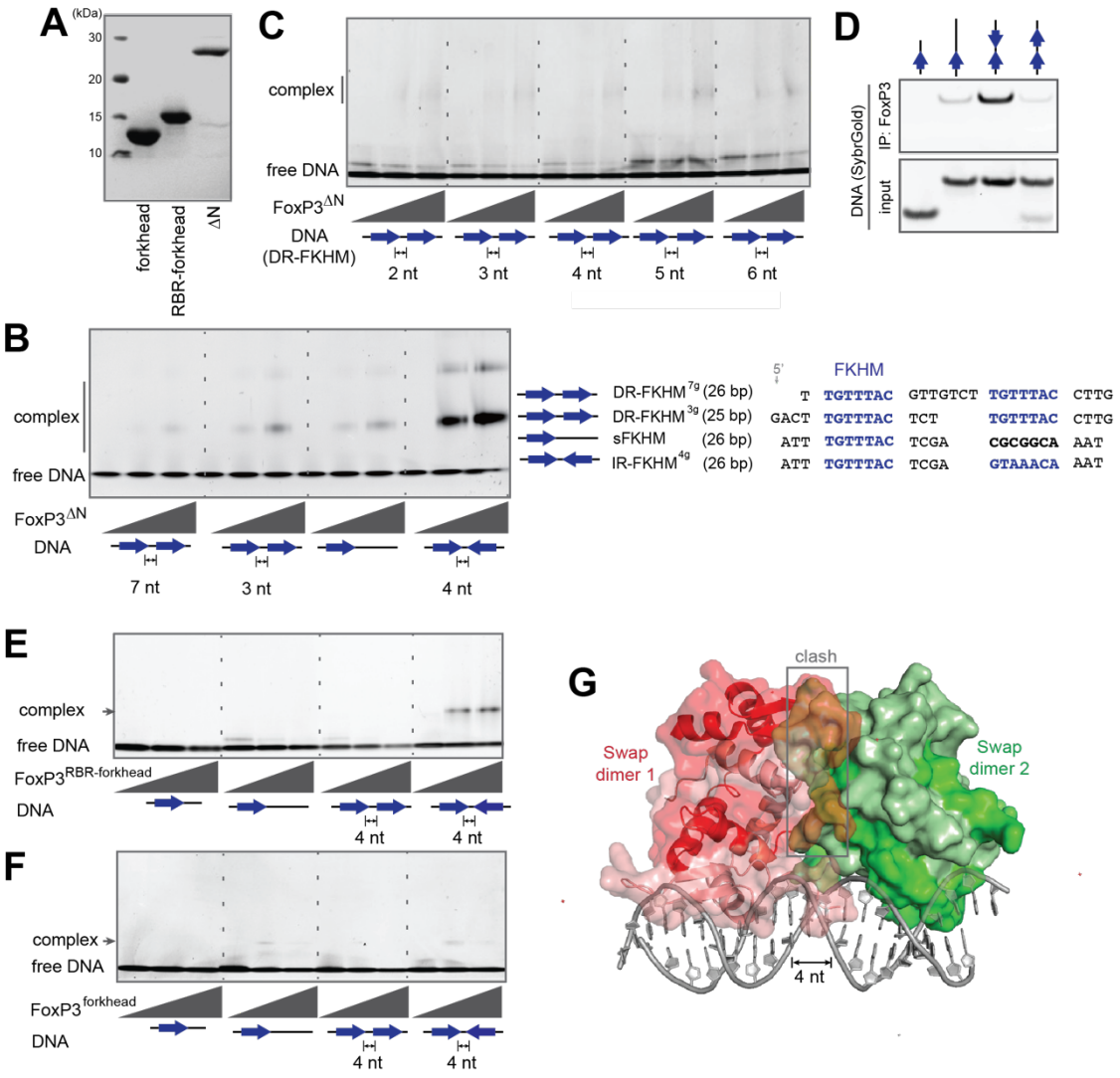

Figure S1. FoxP3$^{\Delta N}$ and FoxP3$^{RBR\text{-}forkhead}$, but not FoxP3^{forkhead}, preferentially binds IR-FKHM^{4g}. Related to Figure 1.

A. SDS-PAGE analysis of recombinant proteins FoxP3$^{\Delta N}$, FoxP3$^{RBR\text{-}forkhead}$, and FoxP3^{forkhead} purified from *E. coli*.

B. EMSA of FoxP3$^{\Delta N}$ (0, 0.8 and 1.6 μM) using four DNA oligos (0.2 μM) with indicated DNA sequences. Sybr Gold stain was used to visualize DNA.

C. EMSA of FoxP3$^{\Delta N}$ (0, 0.4 and 0.8 μM) with DNA containing direct repeats (DR) of FKHM with various gap sizes (0.2 μM).

D. DNA specificity of full-length FoxP3 as measured by FoxP3 pull-down. HA-tagged FoxP3 was ectopically expressed in 293T cells and purified by anti-HA immunoprecipitation (IP). DNA was added to FoxP3 bound to beads and further purified to analyze FoxP3–DNA interaction. DNA in the eluate was analyzed by Sybr Gold stain.

E. EMSA of FoxP3$^{RBR\text{-}forkhead}$ (0, 0.4 and 0.8 μM) using four DNA oligos (0.2 μM) with different FKHM arrangements.

F. EMSA of FoxP3^{forkhead} (0, 0.8 and 1.6 μM) using four DNA oligos (0.2 μM) with different FKHM arrangements.

G. Modeling of the two swap dimers bound to IR-FKHM^{4g}, where each dimer occupies a FKHM facing each other. Modeling suggests that the two swap dimers cannot simultaneously occupy the two FKHMs due to steric clash.

Data in (B-F) are representative of at least three independent experiments.

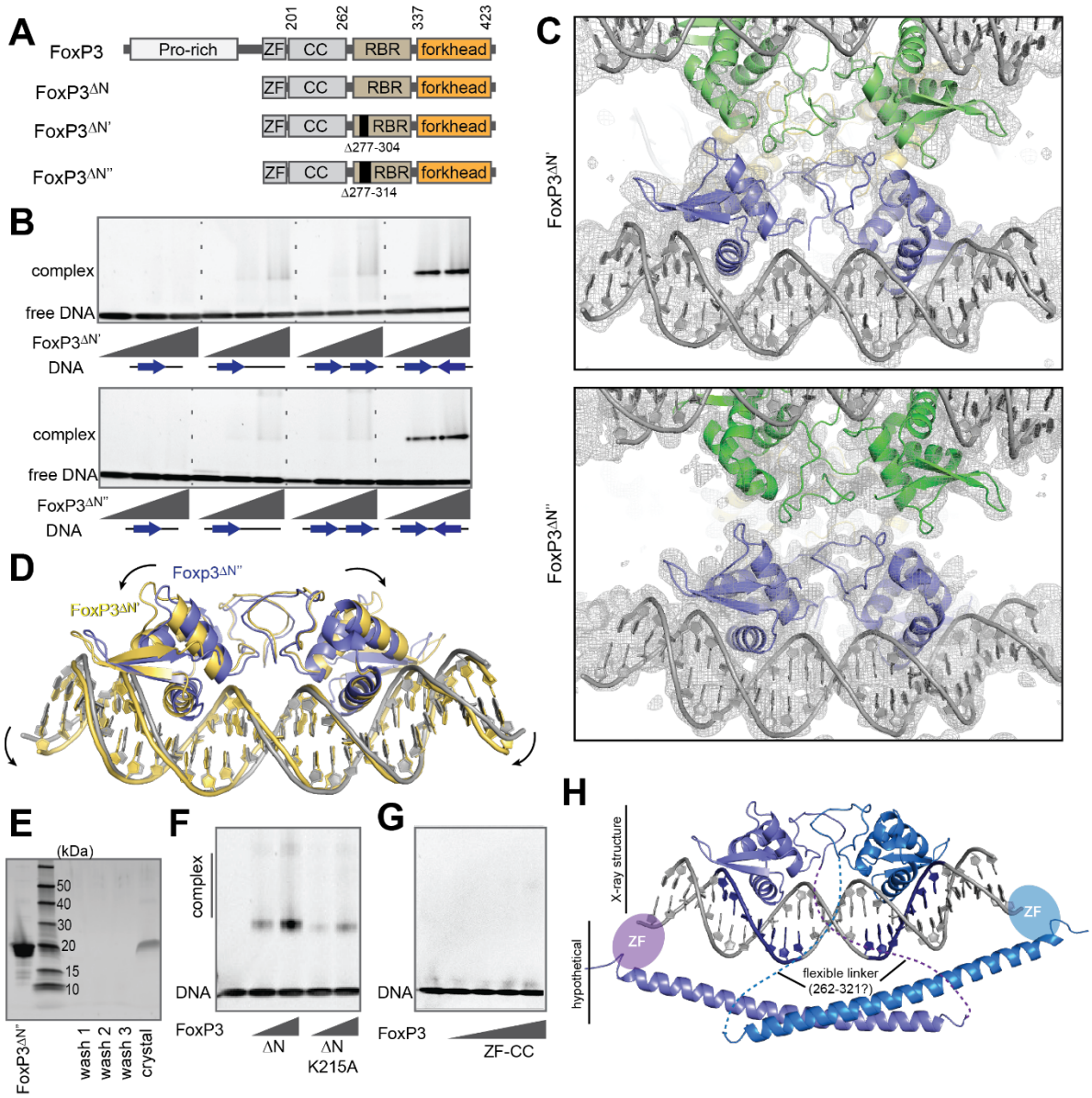

Figure S2 Crystal structures of FoxP3 in complex with IR-FKHM^{4g}. Related to Figure 1.

A. Crystallization constructs FoxP3$^{\Delta N'}$ and FoxP3$^{\Delta N''}$, where residues 277-304 and 277-314 in the RBR linker, respectively, are deleted for crystallization.

B. EMSA of FoxP3$^{\Delta N'}$ and FoxP3$^{\Delta N''}$ (0, 0.4 and 0.8 μM) using four DNA oligos (0.2 μM) with different FKHM arrangements. FoxP3$^{\Delta N'}$ and FoxP3$^{\Delta N''}$ also prefer IR-FKHM^{4g}, as with FoxP3$^{\Delta N}$.

C. Composite omit $2F_o$-F_c map for the crystal structures of FoxP3$^{\Delta N'}$ and FoxP3$^{\Delta N''}$ (sigma=1). Purple proteins are one H-H dimer (bottom), while green (top) and yellow (back) proteins are two other H-H dimers related by the 3-fold crystallographic symmetry. Note that the two monomers within each H-H dimer were refined with crystallographic 2-fold symmetry using the reflection data processed with $P6_322$ symmetry. See Methods for details.

D. Comparison of the FoxP3$^{\Delta N'}$ (yellow) and FoxP3$^{\Delta N''}$ (purple) structures showing slightly altered interaction between monomers and DNA conformations.
E. SDS-PAGE analysis of the crystal (FoxP3$^{\Delta N''}$) showing that the protein is not proteolyzed.
F. EMSA of FoxP3$^{\Delta N}$ (0, 0.4 and 0.8 μM) with and without K215A mutation in ZF. DNA with IR-FKHM^{4g} was used. K215 is a highly conserved Lys that in related C2H2-type ZF proteins is involved in DNA binding.
G. EMSA of FoxP3$^{ZF\text{-}CC}$ (0, 0.5, 1, 2 and 4 μM) using DNA with IR-FKHM^{4g}. Note that DNA binding is barely detectable even with 4 μM of FoxP3$^{ZF\text{-}CC}$.
H. A model of how FoxP3 binds DNA. While ZF and CC could not be resolved in either crystal structure, our data suggest that ZF contributes to DNA binding and that ZF can bind nearby sites on DNA. The locations of ZF and CC relative to forkhead are likely heterogeneous, as evidenced by the lack of electron density for ZF and CC in either of our crystal structures. This is possible because ZF and CC are tethered to forkhead through a long RBR linker, the majority of which (residues 262-321) is also unresolved in the crystal structure and likely flexible. Note that a flexible, a 60-amino acid-long linker is long enough to wrap around DNA. Based on these data, we propose an overall architecture of FoxP3 where the H-H dimer of the forkhead domain forms a primary DNA binding unit, while two ZFs form a secondary binding unit flexibly tethered to the primary unit.

Data in (B, F and G) are representative of at least three independent experiments.

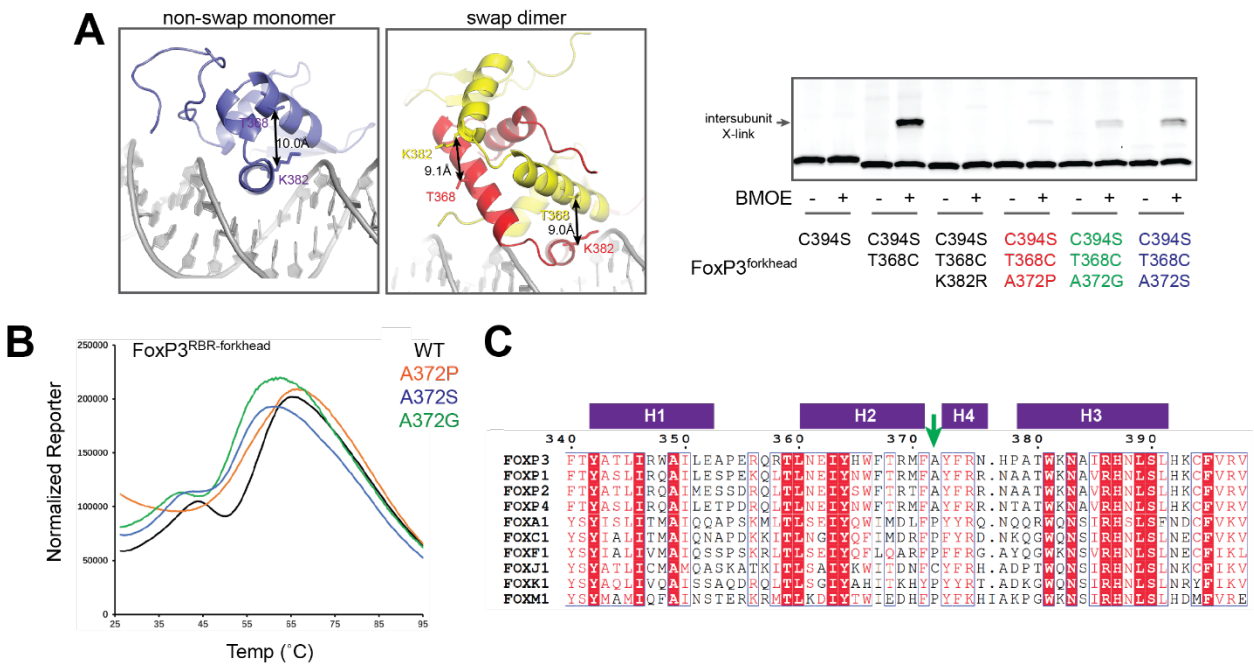

Figure S3. Effect of A372 mutations on swap dimerization and thermal stability. Related to Figure 2.

A. Protein-protein crosslinking (X-linking) to examine the effect of A372 mutations on swap-dimerization. In order to design swap dimer-specific X-linking construct, we introduced C394S, which eliminates background X-linking by BMOE (bifunctional crosslinker that reacts with Cys or Lys). Additionally, we mutated T368 to Cys, which would lead to inter-subunit X-linking between T368C and K382 in the swap dimer, but intra-subunit X-linking in the non-swap monomer. Upon treatment with BMOE, we found that FoxP3^{forkhead} forms inter-subunit X-link in a manner that depends on T368C and K382 (right, lanes 1-6), consistent with its swap-dimeric structure. Introduction of A372P, A372G or A372S reduced the level of inter-subunit X-linking (right, lanes 7-12), suggesting that these mutations suppress swap dimerization.

B. Thermal shift assay showing the reporter fluorescence level with increasing temperature. FoxP3$^{RBR\text{-}forkhead}$ with and without mutations in A372 were compared. Even though A372 mutations do not alter the monomeric state of FoxP3$^{RBR\text{-}forkhead}$ (Figure 2D), A372P shows a significantly altered melting curve compared to WT, A372G or A372S. This result suggests that A372P, but not A372G or A372S, have a negative impact on the thermal stability of FoxP3 independent of its ability to suppress swap dimerization.

C. Sequence alignment of forkhead TFs showing conservation of Ala at the junction of H2 and H4 (green arrow, position 372 in FoxP3 numbering) within the FoxP family. Most forkhead TFs have Pro at the equivalent position although Cys was also observed for FoxJ1.

Data in (A-B) are representative of at least three independent experiments.

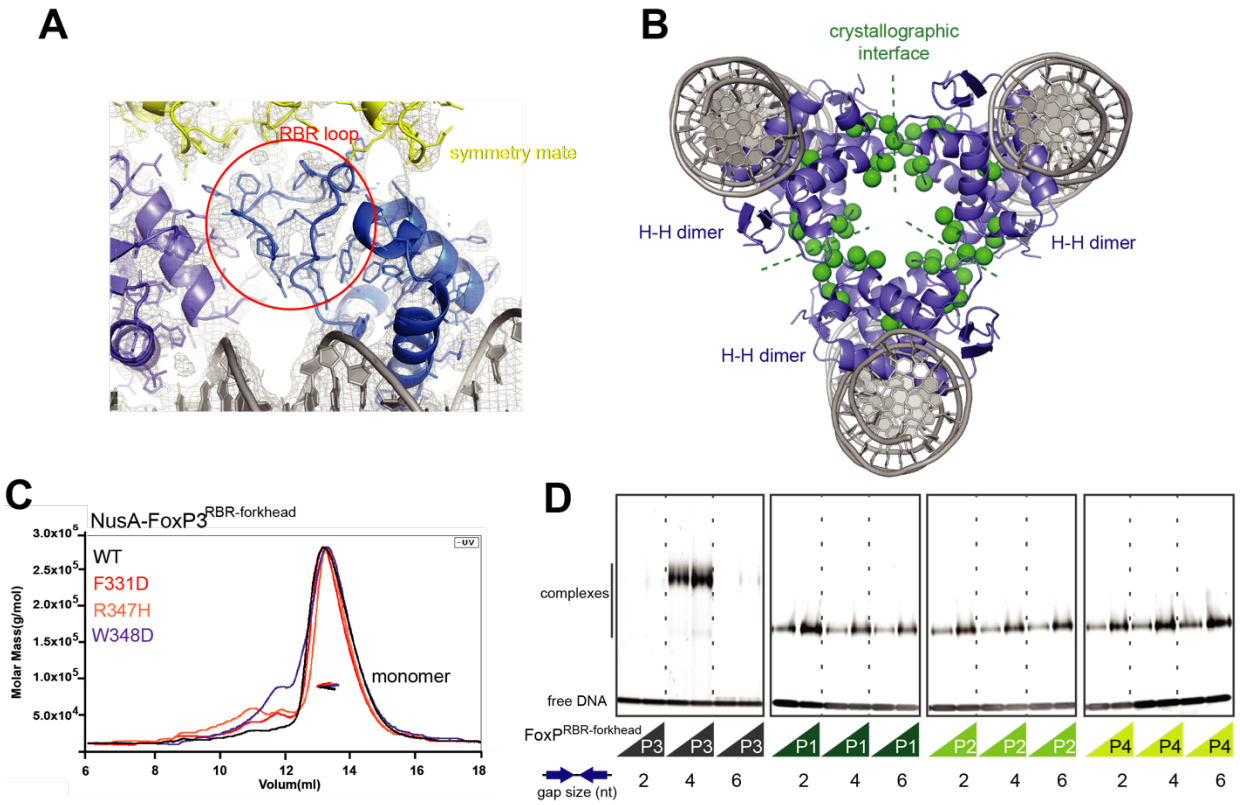

Figure S4. Crystallographic packing of FoxP3 and DNA specificity of FoxP1-4. Related to Figure 3.

A. 2Fo-Fc map near the RBR loop. Symmetry mate related by the 3-fold rotation axis is shown in yellow.
B. Crystal packing of FoxP3 looking down the 3-fold rotation axis. Hydrophobic residues in the RBR loop (indicated in Figure 3A) are shown in green spheres.
C. SEC-MALS of NusA-tagged FoxP3$^{RBR\text{-}forkhead}$ WT and three H-H interface mutants (F331D, R347H and W348D), all showing that they exist predominantly as a monomer.
D. EMSA of NusA-tagged FoxP1-4 (0.4 and 0.8 μM) using DNA oligos (0.2 μM) harboring IR-FKHM with a 2, 4 and 6 nt gap. All proteins were RBR-forkhead domains fused with NusA.

Data in (C and D) are representative of at least two independent experiments.

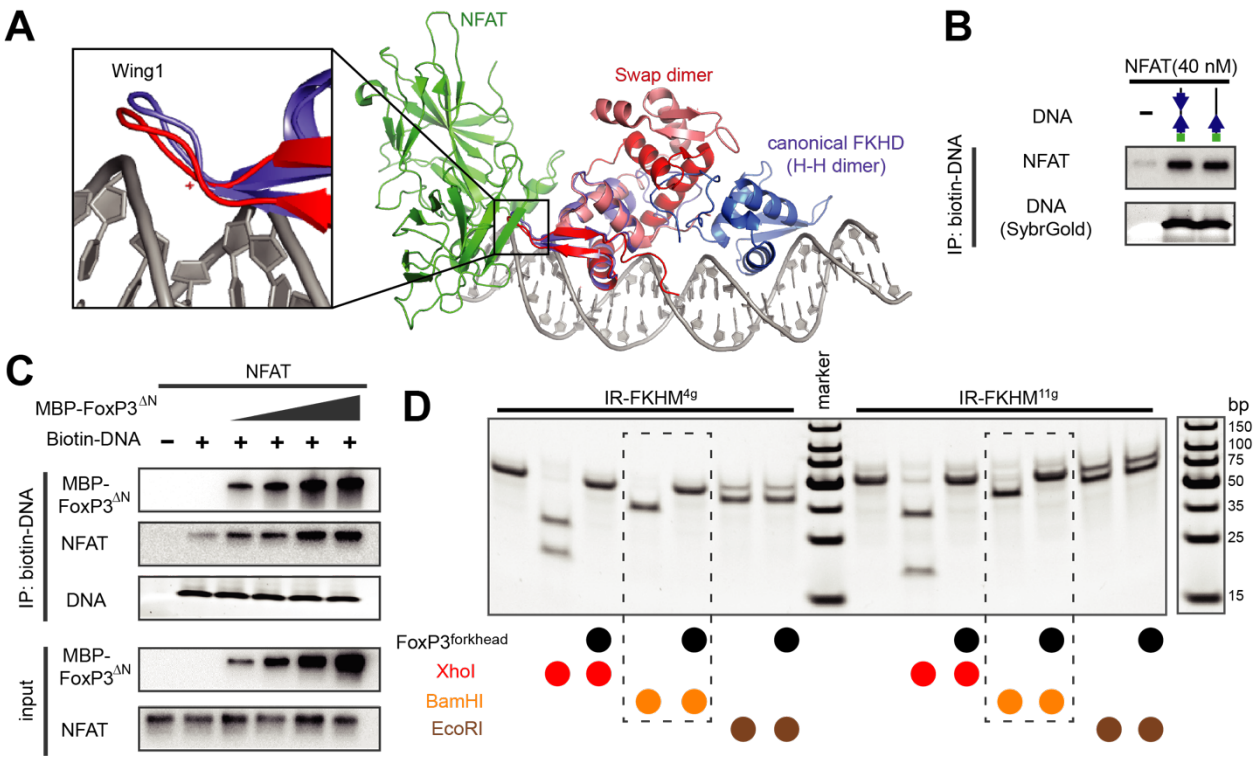

Figure S5. FoxP3–DNA interaction in the presence of NFAT. Related to Figure 4.

A. Overlay of the swap dimeric and non-swap monomeric FoxP3, showing that the NFAT interface of FoxP3 (wing 1) is nearly identical in both structures. Note that the structure of NFAT (green) was determined in complex with the swap dimer (PDB: 3QRF).

B. IR-FKHM^{4g} and sFKHM DNA oligos have equivalent affinity for NFAT^{RHR} in the absence of FoxP3. Biotinylated DNA (0.2 μM) was incubated with NFAT^{RHR} (40 nM) and were subjected to streptavidin pull-down.

C. Effect of FoxP3 on NFAT–DNA interaction. NFAT^{RHR} (8 nM) and biotinylated DNA (0.2 μM) were incubated with an increasing concentration of FoxP3$^{\Delta N}$ (0.1, 0.2, 0.4, 0.8 μM) and were subjected to streptavidin pull-down. DNA contains the IR-FKHM^{4g} and the NFAT consensus site as in Figure 4A. Both FoxP3$^{\Delta N}$ and NFAT^{RHR} were purified from recombinant expression in *E. coli*.

D. Restriction enzyme protection assay with FoxP3^{forkhead} (6.4 μM) in the presence of NFAT^{RHR} (0.4 μM). The mutant A372S was used to ensure that forkhead forms the non-swap conformation. Experiments were performed as in Figure 4D. The result shows that FoxP3^{forkhead} (A372S) binds IR-FKHM^{11g} with individual forkhead occupying each FKHM (as in model (i) in Figure 4C). This differs from FoxP3$^{\Delta N}$, which binds IR-FKHM^{11g} as a H-H dimer (as in model (ii) in Figure 4C).

Data in (B-D) are representative of at least two independent experiments.

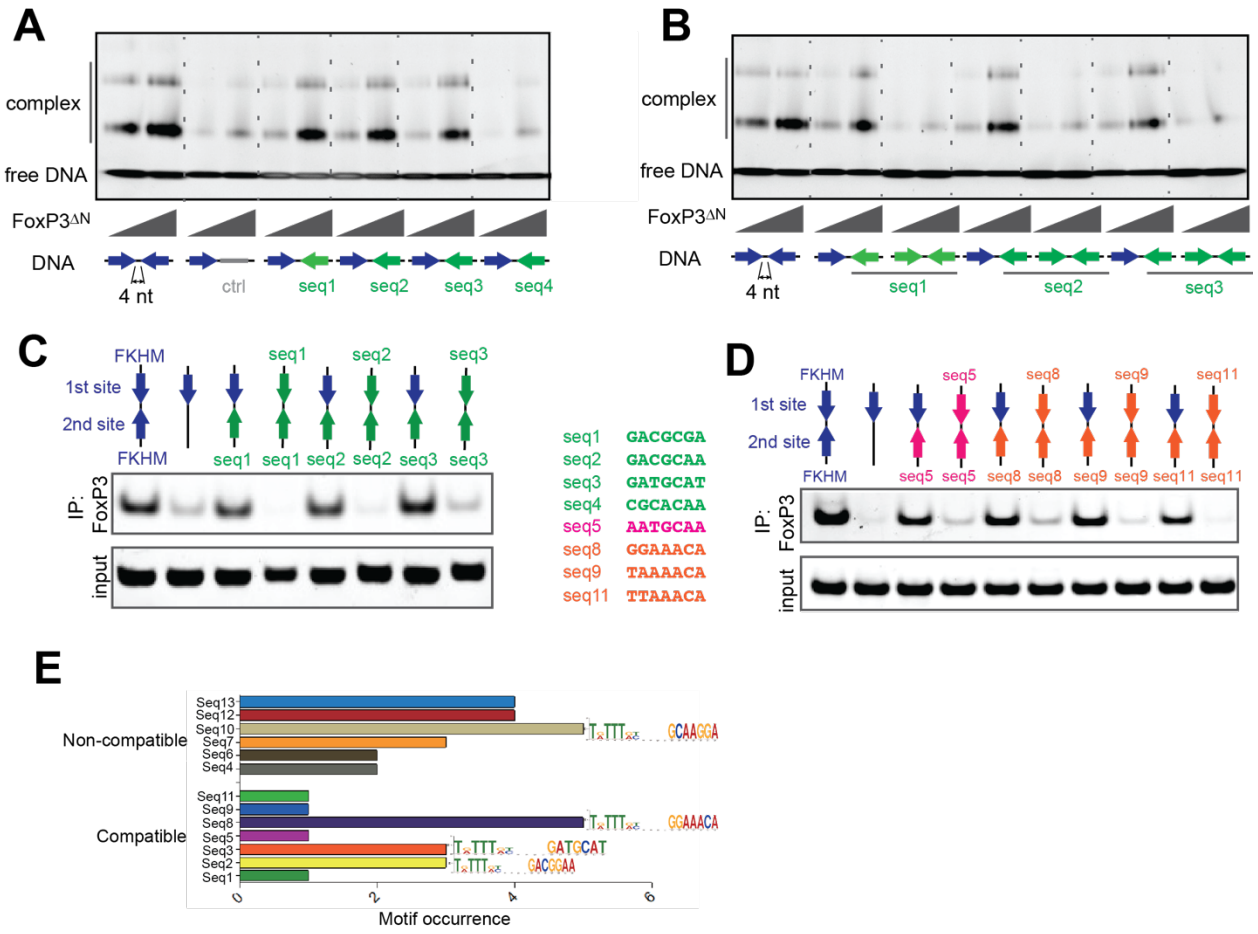

Figure S6. Head-to-head dimerization enables FoxP3 to recognize diverse sequences. Related to Figure 5.

A. EMSA of FoxP3$^{\Delta N}$ (0.4 and 0.8 μM) using DNA containing IR-FKHM^{4g} or FKHM paired with seq1-4 (from Figure 5C).
B. EMSA of FoxP3$^{\Delta N}$ (0.4 and 0.8 μM) using DNA containing IR-FKHM^{4g} or seq1-3 in inverted repeat with 4 nt gaps.
C. FoxP3 interaction with DNA harboring seq1-3 paired with FKHM or inverted repeats of seq1-3. 4 nt gap was used for all.
D. FoxP3 interaction with DNA harboring seq5/8/9/11 (from Figure 5D) in inverted repeats *vs.* those paired with FKHM.
E. Occurrence of compatible and non-compatible dimers in FoxP3 ChIP-seq binding sites that include an FKHM (n=548). Motif occurrences were counted with a FIMO p-value<10^{-5} and score greater than 12.

Data in (A-D) are representative of at least three independent experiments.

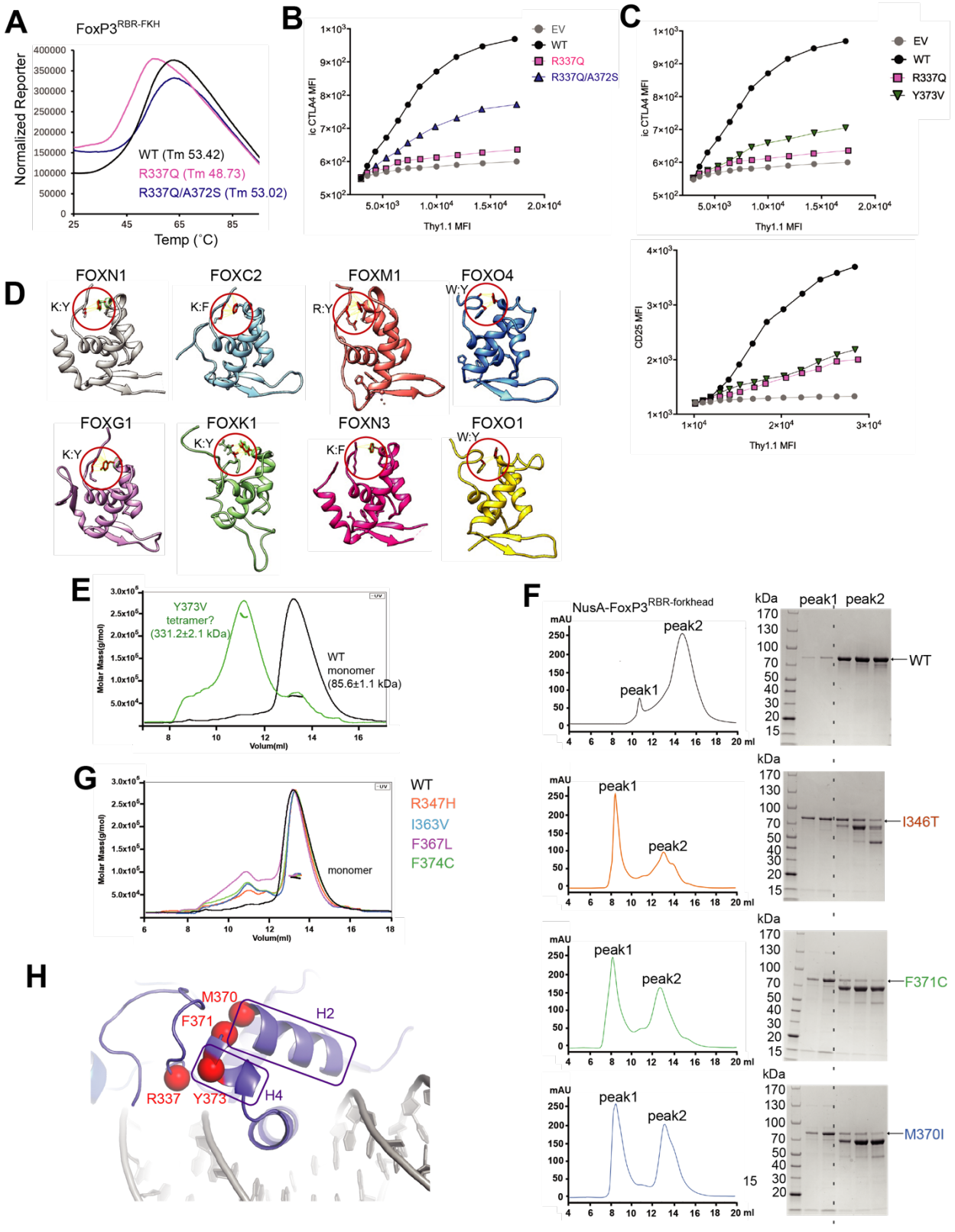

Figure S7. Other IPEX mutations near the H2/H4 junctions can also cause folding errors. Related to Figure 7.

A. Thermal shift assay showing the reporter fluorescence level with increasing temperature. FoxP3 WT, R337Q and R337Q/A372S were compared.
B. Transcriptional activity of FoxP3 as measured by CTLA4 level. The effects of R337Q, either alone or in combination with the swap-suppressive mutation A372S, were examined.
C. Transcriptional activity of FoxP3 with R337Q or Y373V. Experiments were performed as in Figure 2C.
D. Structures of other forkhead proteins highlighting two residues equivalent to R337 and Y373 in FoxP3. In all cases, these two residues are in close proximity with the potential of forming pi–cation and pi-pi interactions.
E. SEC-MALS of NusA-tagged $FoxP3^{RBR\text{-}forkhead}$ (WT and Y373V).
F. SEC profile of NusA-tagged $FoxP3^{RBR\text{-}forkhead}$ (WT, I346T, F371C and M370I). For each protein, SEC fractions corresponding to peaks 1 and 2 were analyzed by SDS-PAGE. Superdex 200 Increase 10/300 column was used for SEC, where void peak is at ~8 ml.
G. SEC-MALS of NusA-tagged $FoxP3^{RBR\text{-}forkhead}$ WT and four IPEX mutations R347H, I363V, F367L and F374C, showing that these proteins predominantly exist as monomers.
H. Locations of folding-disruptive IPEX mutations. Nine IPEX mutations within the forkhead domain of FoxP3 were analyzed and four mutations (R337Q, M370I, F371C, Y373V) were found to disrupt the monomeric state of $FoxP3^{RBR\text{-}forkhead}$. Mapping of these mutations onto the FoxP3 structure (non-swap conformation) revealed that they were clustered near the junction of H2 and H4.

Data are presented as at least two to three independent experiments.

Table S1. Data collection and refinement statistics. Related to Figure 1.

FoxP3$^{\Delta N''}$-DNA	
Data collection	
PDB ID	7TDX
Wavelength (Å)	0.97910
Spacegroup	P 63 2 2
Cell dimensions	
a, b, c (Å)	89.3605, 89.3605, 175.928
α, β, γ (°)	90, 90, 120
Resolution (Å)	46.77-3.1 (3.21-3.1)
Rmerge	0.218 (0.847)
I/σI	15.1 (3.8)
Completeness (%)	99.7 (99.9)
Redundancy	19.0 (20.3)
CC1/2	0.994 (0.996)
Refinement	
Resolution (Å)	46.77-3.1 (3.21-3.1)
No. of reflections	7805 (776)
Rwork/Rfree	0.2977/0.3148
No. of atoms	1349
Protein	778
DNA	571
Water	0
Average B-factors (Å^2)	137.99
RMSDs from ideal	
Bond lengths (Å)	0.006
Bond angles (°)	1.19
Ramachandran plot (%)	
Favored	95.45
Allowed	4.55
Disallowed	0
Values in parentheses are for the highest-resolution shell.	

FoxP3$^{\Delta N'}$-DNA	
Data collection	
PDB ID	7TDW
Wavelength (Å)	0.97918
Spacegroup	P 63 2 2
Cell dimensions	
a, b, c (Å)	99.092, 99.092, 179.398
α, β, γ (°)	90, 90, 120
Resolution (Å)	72.8-4.0 (4.14-4.0)
Rmerge	0.224 (2.213)
I/σI	7.4 (1.8)

Completeness (%)	99.7 (99.9)
Redundancy	12.2 (13.1)
CC1/2	1 (0.935)
Refinement	
Resolution (Å)	72.8-4.0 (4.14-4.0)
No. of reflections	4178 (398)
Rwork/Rfree	0.3347/0.3592
No. of atoms	1349
Protein	778
DNA	571
Water	0
Average B-factors (Å^2)	269.17
RMSDs from ideal	
Bond lengths (Å)	0.004
Bond angles (°)	0.59
Ramachandran plot (%)	
Favored	94.32
Allowed	5.68
Disallowed	0
Values in parentheses are for the highest-resolution shell.	

Table S2. **Sequences of dsDNAs and Biotin-dsDNAs. Related to STAR methods.**

dsDNAs	sequences (5'-3')
IR-FKHM^{4g}(24bp)	ATT **TGTTTAC** TCGA **GTAAACA** AAT
IR-FKHM^{4g}(28bp)	AAATT **TGTTTAC** TCGA **GTAAACA** AATTT
IR-FKHM^{4g}(31bp)	TTAGGAAAATT **TGTTTAC** TCGA **GTAAACA** AA
IR-FKHM^{4g}(47bp)	TTAGGAAAATT **TGTTTAC** TCGA **GTAAACA** GTGGATCCGAATTC ATAT
IR-FKHM^{2g}	TTA GGAAA ATT **TGTTTAC** TC **GTAAACA** AA
IR-FKHM^{3g}	TTA GGAAA ATT **TGTTTAC** TCG **GTAAACA** AA
IR-FKHM^{5g}	TTA GGAAA ATT **TGTTTAC** TCAGA **GTAAACA** AA
IR-FKHM^{6g}	TTA GGAAA ATT **TGTTTAC** TCAGGA **GTAAACA** AA
IR-FKHM^{11g}	TTAGGAAAATT**TGTTTAC**TCGAGTGTACG**GTAAACA**GTGGAT CCGAATTC ATAT
sFKHM(22bp)	TTA GGAAA ATT **TGTTTAC** TCGA
sFKHM(24bp)	ATT **TGTTTAC** TCGA **CGCGGCA** AAT
sFKHM(31bp)	TTAGGAAAATT **TGTTTAC** TCGA CGCGGCA AA
DR-FKHM^{2g}	TTAGGAAAATT **TGTTTAC** TC **TGTTTAC** AA
DR-FKHM^{3g}	TTAGGAAAATT **TGTTTAC** TCG **TGTTTAC** AA
DR-FKHM^{4g}	TTAGGAAAATT **TGTTTAC** TCGA **TGTTTAC**
DR-FKHM^{5g}	TTAGGAAAATT **TGTTTAC** TCAGA **TGTTTAC** AA
DR-FKHM^{6g}	TTAGGAAAATT **TGTTTAC** TCAGGA **TGTTTAC** AA
DR-FKHM^{3g}(25bp)	GACT**TGTTTAC**TCT**TGTTTAC**CTTG
DR-FKHM^{7g}(26bp)	T**TGTTTAC**GTTGTCT**TGTTTAC**CTTG
FKHM-seq1	ATT **TGTTTAC** TCGA **GACGCGA** AAT
FKHM-seq2	ATT **TGTTTAC** TCGA **GACGCAA** AAT
FKHM-seq3	ATT **TGTTTAC** TCGA **GATGCAT** CAT
FKHM-seq4	ATT **TGTTTAC** TCGA **CGCACAA** AAT
IR-seq1	ATT **TCGCGTC** TCGA **GACGCGA** AAT
IR-seq2	ATT **TTGCGTC** TCGA **GACGCAA** AAT
IR-seq3	ATG **ATGCATC** TCGA **GATGCAT** CAT
FKHM-seq5	TTAGGAAAATT **TGTTTAC** TCGA **AATGCAA** AA
FKHM-seq6	TTAGGAAAATT **TGTTTAC** TCGA **CCTTGTT** AA
FKHM-seq7	TTAGGAAAATT **TGTTTAC** TCGA **GAGGAGG** AA
FKHM-seq8	TTAGGAAAATT **TGTTTAC** TCGA **GGAAACA** AA
FKHM-seq9	TTAGGAAAATT **TGTTTAC** TCGA **TAAAACA** AA
FKHM-seq10	TTAGGAAAATT **TGTTTAC** TCGA **GCAAGGA** AA
FKHM-seq11	TTAGGAAAATT **TGTTTAC** TCGA **TTAAACA** AA
FKHM-seq12	TTAGGAAAATT **TGTTTAC** TCGA **TAGCAGG** AA
FKHM-seq13	TTAGGAAAATT **TGTTTAC** TCGA **TTCTTCA** AA
IR-seq5	TTAGGAAAATT **TTGCATT** TCGA **AATGCAA** AA
IR-seq8	TTAGGAAAATT **TGTTTCC** TCGA **GGAAACA** AA
IR-seq9	TTAGGAAAATT **TGTTTTA** TCGA **TAAAACA** AA
IR-seq11	TTAGGAAAATT **TGTTTAA** TCGA **TTAAACA** AA
Major FKHM-seq5	AAA **TGTTTAC** TAGG **AATGCAA** TGA
minor FKHM-seq5	AAA **TGTTTA**A TAGG **AATGCAA** TGA
Major seq8-seq9	GTT **TGTTTCC** CAGG **TAAAACA** ACC
minor seq8-seq9	GTT **TGTTTCC** CAGG **TA**T**AACA** ACC
Major seq11-seq12	CAG **TGTTTAA** AAGA **TAGCAGG** CTT
minor seq11-seq12	CAG **TA**T**TTAA** AAGA **TG**G**CAGG** CTT
Biotin-IR-FKHM^{4g}	Biotin-TAGGAAAATT **TGTTTAC** TCGA **GTAAACA** GA
Biotin-sFKHM	Biotin-TAGGAAAATT **TGTTTAC** TCGA **CGCGGCA** GA